Journal of
Animal Biology and Veterinary Medicine

JScholar
Fostering Scholarly Communication

Research Article Open Access

Skin Transcriptome Analysis of Sphynx and Haired Sphynx Mutant Cats

Xueting Qu, Wei Ge, Sen Wang, Minghui Zhao, Kunpeng Yuan, Yijun Han, Hao Zhou, Qingdong Luan, Haonan Qi, Ju Sun and Yanbo Yin*

College of Veterinary Medicine, Qingdao Agricultural University, Qingdao 266019, China

***Corresponding author:** Yanbo Yin, College of Veterinary Medicine, Qingdao Agricultural University, Qingdao 266019, China, E-mail: yanboyin2011@163.com

Citation: Xueting Qu, Wei Ge, Sen Wang, Minghui Zhao, Kunpeng Yuan, et al., (2022) Skin Transcriptome Analysis of Sphynx and Haired Sphynx Mutant Cats. J Anim Biol Vet 2: 1-21.

Abstract

Background: Hairless cats are suitable models for studying skin, hair, and other related diseases. To detect differences in skin transcription between Sphynx and hair Sphynx mutant cats, and to explore the genes related to hair regulation, we extracted RNA from skin samples and performed transcriptional analysis using RNA-seq.

Results:132 differentially expressed genes were identified in the domestic cat, Sphynx, and hair Sphynx mutant cat, and histological differences among the four groups of cats were found in hematoxylin-eosin staining.

Conclusions: The candidate genes identified in this study may be potential regulators of hair length in cats. These consequences will deepen our understanding of hairless cats and lay the foundation for their use as good animal models.

Keywords: Skin; Sphynx cat; Transcriptome

©2022 The Authors. Published by the JScholar under the terms of the Creative Commons Attribution License http://creativecommons.org/licenses/by/3.0/, which permits unrestricted use, provided the original author and source are credited.

Introduction

Our laboratory has bred two Sphynx cats, which produced cats with back-curled hair, small body size, no obvious genetic disorders, a docile and active character, and a similar appearance to the Devon cat. This observed phenomenon has not been studied to date. Therefore, we used second-generation high-throughput sequencing methods to understand the differences between the two.

The presence or absence of skin hair is the most significant difference between haired Sphynx mutant cats and Sphynx. According to the concept of forwarding genetics, the hair growth of haired Sphynx mutant cats is related to the mutant gene function. Previous studies have determined the genetic basis of several fur colors in cats [1,2]. FGF5 [3,4] is the primary gene that controls fur length, but relatively little is known about the genes affecting fur growth and curl variation. Hair is a unique structural feature of mammals, and it controls the homeostasis of the body as well as the integration of cells and tissues. Previous studies on dog [5], mouse [6], and rat [7] have determined that keratin 71 (KRT71) polymorphism causes curl/wave phenotype.

Moreover, the mutations of Sphynx and Devon Rex are known in KRT71 [7]. The long-term signal pathways involved in hair genesis are mainly activated by Wnt [8], Notch [9], MAPK/sonic hedgehog (SHH) [10], and TGF- β family member [11], but the mechanism is not certain. The understanding of hair is not easy because hair molecules are formed differently at each stage of a cycle [12,13]. At present, there are many speculations about the initial molecular signals that promote dermis formation in hair formation, but no definite conclusion has been drawn.

The epidermis of cats is comprised of the stratum corneum, granular layer, spinous layer, and basal layer. Montagna [14] pointed out that the thickness of the mammalian epidermis is related to the density of the body coat, while the thickness and complexity of the dermis depend mostly on the epidermis thickness.

The process of hair formation is complex in mechanism and relates to various signal channels. Hair-inductive capacity lies within the dermis, which has been demonstrated in "cut-and-paste" tissue recombination experiments [15]. Moreover, it is known that the widespread Wnt signal activity in the epidermis of (E) 12.5 precedes hair follicle (HF) formation and is essential for HF induction [16]. This signal acts on the epidermis and induces placode (Pc) formation on E14.0 [17], thus producing the "first epithelial signal" acting on the lower fibroblasts. Despite various speculations on the initial molecule signals promoting dermal formation during hair genesis [18], no definite conclusion has been drawn so far.

Spacing Keratin (keratin, K) gene is the principal structural protein in mammalian skin epithelial cells. The promoters of different keratins are transcribed and expressed in specific epithelial structures such as hair follicles [19]. For example, the promoters of K14 and K5 [20,21] are mainly expressed in the basal layer of the epidermis and the outer root sheath of hair follicles; K1 and K10 [22,23] promoters are targeted at the end of epidermal keratin cell differentiation; and K15 [24] promoters are targeted in hair follicle epithelial stem cells. It represents an ideal tool for related experiments. At present, 54 functional keratins intermediate filament gene (Krts) families have been found to be located in human chromosomes 12 and 17 [25] with high homology. For human beings, there are various diseases related to hair, such as alopecia, atrichia, etc [26], most of which have not been solved effectively. In addition, conventional animals adopted for studying human-related hair diseases such as nude mice and hairless guinea pigs do not meet certain requirements. Therefore, as naturally mutated hairless individuals, hairless Sphynx can be used in establishing animal models to study hair-related diseases of human beings.

Materials and Methods

Animals

Ethical Statement

All the cats were from Qingdao Bolong Experimental Animal Co., Ltd., and were kept in the same environment. The cats were given access to a variety of toys and scratching posts to enrich their behavior. Throughout the experiment, the Cats were fed a commercial dry diet (Whiskas Meaty Selections, Mars, Inc., Mattoon, IL) to maintain body weight, and water was available ad lithium. All the cats received routine immunisation procedures.

Specimen collection, preparation, and histological examination

All operations were performed using the anesthetized cat described in the standard operating procedure (SOP). A tissue sample (1cm^2) was derived from the neck of each cat after shaving for histological analysis. The skin sample was fixed with 4% paraformaldehyde solution. Then, the cross-section of the fixed sample was rinsed with tap water, dehydrated with ethanol series, cleaned with xylene, and embedded in paraffin. The specimen section with a thickness of 5 microns was achieved using a Leica RM2235 slicer (Leica, Germany). The fixed and paraffin-embedded samples were stained with HE in both horizontal and vertical sections, and were detected and photographed using an Olympus CX31 biological microscope (Olympus Optical Company, Tokyo, Japan).

cDNA library construction and sequencing

Under standard anesthesia, neck skin samples (removal of hair coat) from all four groups of cats were immediately frozen in liquid nitrogen and stored at −80°C for RNA extraction. According to the manufacturer's instructions, total RNA was extracted from skin samples of Sphynx male cats (designated as SFG1, SFG2, SFG3), Sphynx female cats (designated as SFM1, SFM2, SFM3), Sphynx mutant cats (designated as SFTB1, SFTB2, SFTB3) and domestic cats (designated as CK1, CK2, CK3) using Trizol reagent (Invitrogen, Carlsbad, CA, USA). Then, the samples were forwarded to Biomarker Technologies Corporation, Beijing. The quality of RNA was evaluated using Agilent 2100 breathalyzer (Agilent, Santa Clara, CA, USA). mRNA was purified, fragmented, and transformed into cDNA. The adaptor was connected to the end of the double-stranded cDNA. Based on the manufacturer's agreement, the Illumina Tru-Seq RNA sample preparation kit (Illumina, San Diego, CA, USA) was used to establish the library by polymerase chain reaction (PCR). Qubit2.0 was used to quantify the constructed library, and Agilent 2100 was used to determine the size of the inserted library. According to the manufacturer's instructions, 12 separate paid libraries were sequenced with Illumina Hi-Seq 2500 (Illumina, San Diego, CA, USA) systems. Clean reads of 6.5 Gb or more of each sample were produced for genome-wide transcription analysis.

Mapping and assembling

The trimmed reads were assembled and mapped to the reference genome (https://www.ncbi.nlm.nih.gov/genome/?term=cat) by performing alignments using the TopHat2 [27] software. The AS and SNPs were analyzed using the Cufflinks [28] and GATK software [29], respectively.

Differential gene expression analysis

The values of fragments per kilobase of transcript per million fragments mapped (FPKM) [27] were generated to identify the expression level of genes in each cat sample. Differential expression analysis was performed with DESeq and R package. The generated new unigenes were used for annotation against the NR [30] Swiss-Prot [31] GO [32] COG [33] KOG [34] PFAM [35] KEGG [36]. The P-value corresponds to a differential gene expression test in which the false discovery rate (FDR) was used to determine the threshold of P-value in multiple tests. We filtered the differentially expressed genes (DEGs) with the standards (Fold Change ≥2 and FDR<0.01). All the DEGs, whose function was analyzed by the gene ontology (GO), were mapped to the GO terms in the database (http://www.Geneontology.org/). The Kyoto Encyclopedia of Genes and Genomes (KEGG) database was used to perform the pathway enrichment analysis of the DEGs. We performed the analysis of the first 20 signaling pathways in KEGG analysis using the KEGG classification enrichment Figure tools on the BMKCloud platform (www.biocloud.net).

qRT-PCR

To verify Illumina sequencing data, 8 DGEs were selected in this study for quantitative RT-PCR (qRT-PCR) analysis.

RNA samples used for qRT-PCR amplification and those used to construct the above RNA-Seq library were the same. Gene-specific primers were designed with Primer 5.0(Table1). Quantitative RT-PCR (BIOER, Hangzhou) was conducted using TransStart Green qPCR SuperMix (TransGen Biotech, Beijing, China) in accordance with the manufacturer's agreement. The following conditions were used for amplification: 94°C for 30s, followed by 40 cycles of 94°C for 5s, 62°C for 35s, and a melt curve stage of 97°C for 10 s, 65°C for 1min, and 97°C for 1s. All reactions were performed at three biological triplicates, and the resulting Ct values were analyzed by a one-way analysis of variance (ANOVA) using the SPSS 19.0 statistical program. The results were expressed as meaning ± standard errors.

Results

Analysis of RNA sequencing results of four groups of cats

Twelve cDNA libraries of a domestic cat (CK1, CK2, CK3), a Sphynx male cat (SFG1, SFG2, SFG3), a Sphynx female cat (SFM1, SFM2, SFM3), and a Sphynx offspring mutant hairy cat (SFTB1, SFTB2, SFTB3) were constructed (figure 1a).

A total of 77.41 Gb Clean data were obtained after removing low-quality reads and adaptor sequences, and the Clean Data of each sample was more significant than 6.23 GB (Q30 ≥ 93.34%) (Table2). Through the expression PCA mapping (figure.1b)

we can see that the four cat samples are distinguished. The distance between biological repeats is relatively close, verifying the biological repeats' consistency and the differences among these groups. The dendrogram of four sample groups showed that the Sphynx hairy mutant cat (SFTB) was closer to the Sphynx male cat (SFG) in the dendrogram, and the domestic cat (CK) was not on the same branch (Fig.1c) as the other three groups of cats.

Figure.1(a)

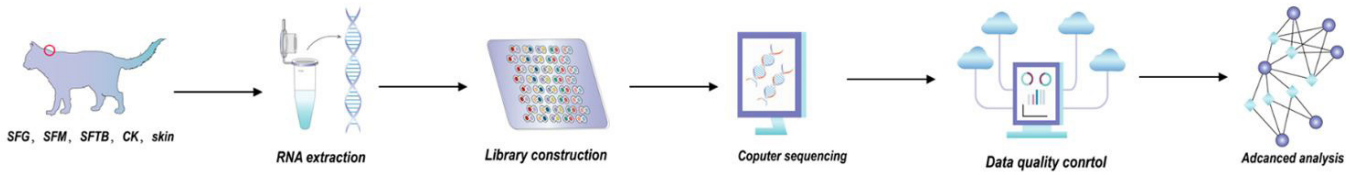


Figure1 (b)

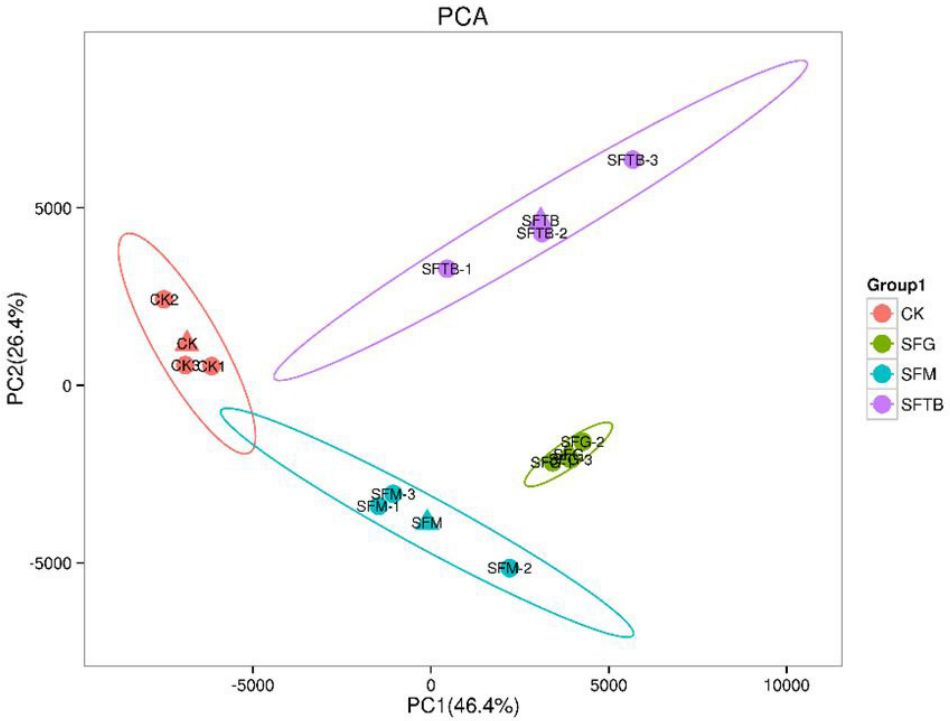


Figure1(c)

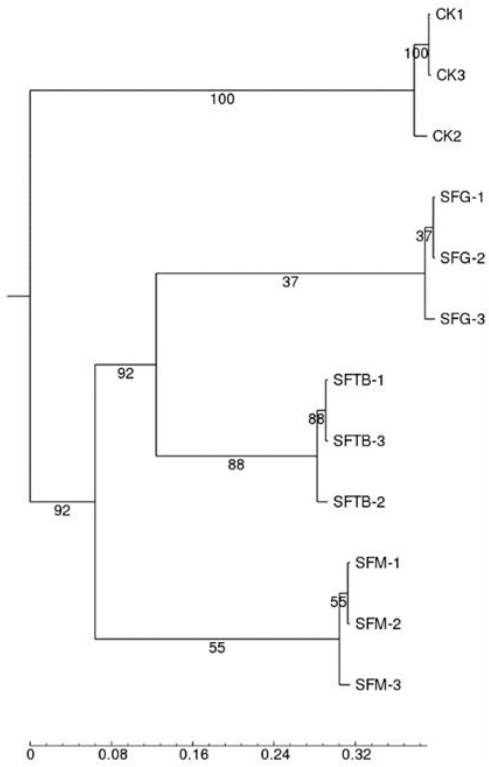


Figure 1: RNA sequencing and sequencing data analysis (a) technology roadmap of RNA sequencing (b) Expression quantity PCA analysis (c) Phylogenetic tree

Comparison of longitudinal sections of human skin in four groups of experimental cats

Longitudinal sections of the hairy group (domestic cat and Sphynx cat) showed a more transparent hair follicle outline after HE staining (Figure.2(a) Figure 2(b) A1 and A2).

The nucleus of the hair follicle was stained blue. In the hairless group (SFM and SFG), the neck skin's longitudinal section was stained with HE and was shown to be significantly more sebaceous glands than the hairy cats (Figure. 2(b) A3 and A4). It was also noted that the cat is a composite hair follicle, like other mammals. The skin thicknesses of SFG, SFM, SFTB, and CK are 1.91mm, 1.95mm, 1.65mm, and 1.24mm, respectively. By sectioning (Fig. 2(b) B1 and B2), the hairy cat's epidermis is significantly thinner than the hairless cat (Fig. 2(b) B3 and B4). However, densely stained particles can be seen, the hairless cats (Fig. 2(b) B3 and B4) are composed of 1-2 layers of granular layer cells, and the cell outline is clear, and the deeply stained particles can be seen. The spinous layer of the hairy cat is composed of 1-2 layers of squamous epithelial cells. In comparison, the hairless cat is composed of 3-4 layers of squamous epithelial cells, which are significantly thicker than the hairy cat.

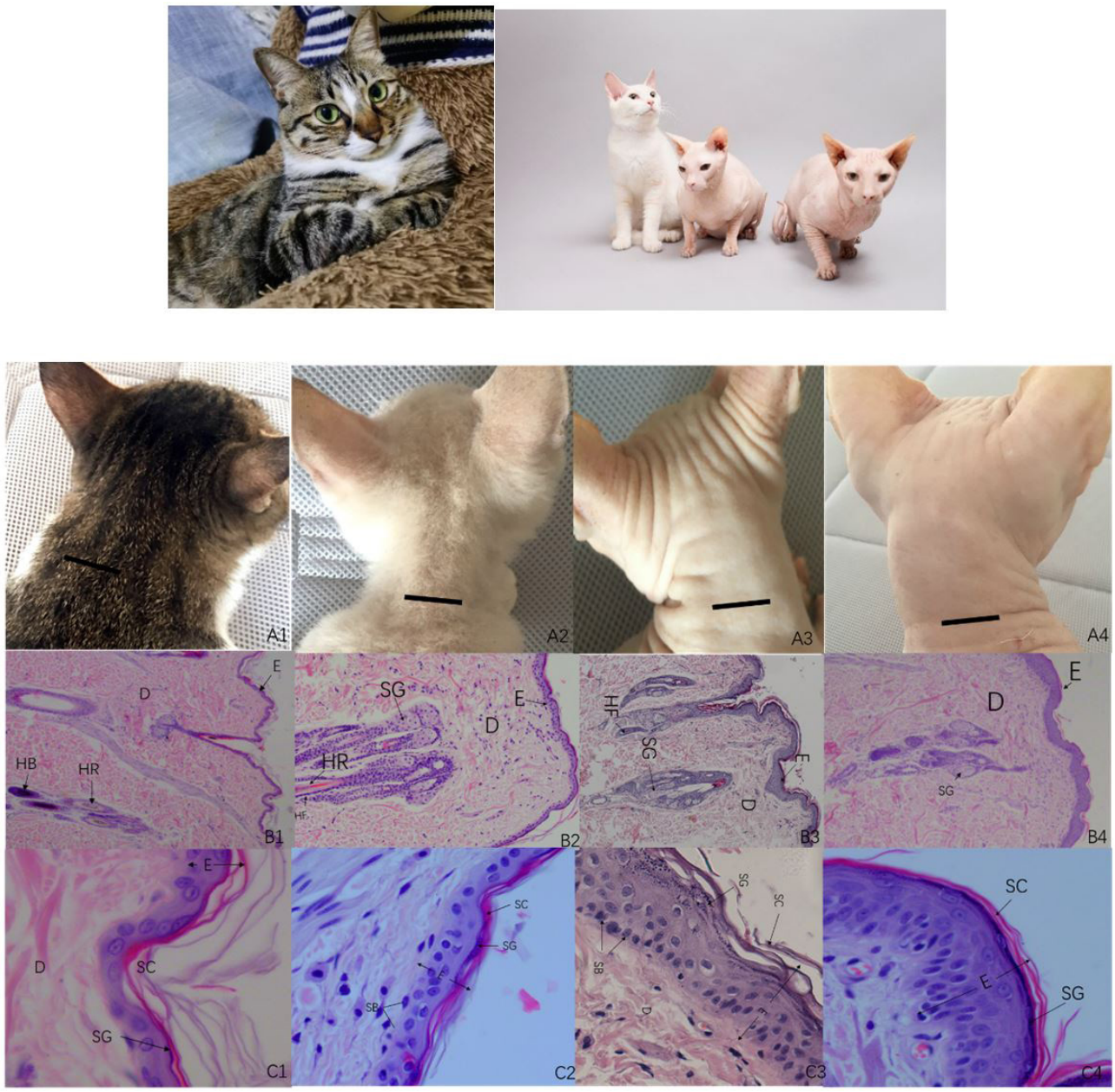


Figure 2: Photos and skin histopathological sections of four groups of cats (a) Four groups of cat photos (b) Skin tissue section. A1: Sampling site of neck skin in domestic cat A2: Sampling site of neck skin in sphinx cats A3: Sampling site of neck skin in sphinx males A4: Sampling site of neck skin of sphinx female (After sampling, the skin of all four groups of experimental cats returned to normal, leaving no scars) B1: domestic cat neck skin. E. epidermis; D. dermis; HR. hair root; HB. hairball B2: sphinx mutation with hairy cat neck skin. E. epidermis; D. dermis; HR. hair root; SG. sebaceous gland B3: sphinx male cat neck skin. E. epidermis; D. dermis; HF. hair follicle; SG. sebaceous gland B4: sphinx female cat neck skin. E. epidermis; D. dermis; SG. a sebaceous gland (magnification 40 times) C1: domestic cat epidermis. E. epidermis; D. dermis; SC. stratum corneum; SG. granule layer C2: sphinx mutation with hairy cat epidermis. E. epidermis; D. Dermis; SC. stratum corneum; SG. granule layer; SB. basal layer C3: sphinx male cat epidermis. E. epidermis; D. dermis; SC. stratum corneum; SG. granule layer; SB. Basal layer C4: Sphinx female cat epidermis.E. epidermis; SC. stratum corneum; SG. granule layer (magnification 400 times)

Results of differential expression analysis of transcriptome genes in Sphynx cat group and domestic cat group

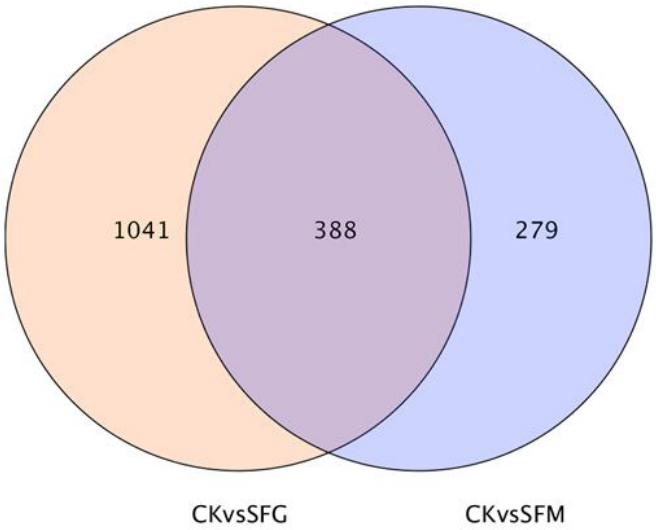
The parameter FDR=0.01 FC=2 was set according to the software DESeq_EBSeq [37] to analyse and compare the two groups CK, SFM, SFG, and SFTB to obtain the number of differential genes (Table 1).

Analysis of the Veen mapping of SFG, SFM, and CK revealed a total of 388 co-expressed DGEs; the first 20 signal pathways (figure.3a) were obtained by analysis of the KEGG database (http://www.genome.jp/kegg/). The DGEs enriched in signal pathways, including ***Wnt signaling pathway, TGF-beta signaling pathway, ECM-receptor interaction, MAPK signaling pathway, P13K-Akt signaling pathway,*** were mainly genes such aa BMP4, FGF5, NOTUM, FGF18, DUPS1. However, there was no significant difference in the expression of these genes. Besides, 388 differentially expressed genes were analyzed by GO (http://metascape.org) analysis (figure.3b) and enriched out dodgy clusters (http://metascape.org) (figure3c).

Parameters	group	DEGs_total	DEGs_up	DEGs_down
DESeq_EBSeq FDR=0.01 FC=2	CK1&CK2&CK3_vs_SFG-1&SFG-2&SFG-3	1429	833	596
	CK1&CK2&CK3_vs_SFM-1&SFM-2&SFM-3	667	328	339
	SFTB-1&SFTB-2&SFTB-3_vs_SFG-1&SFG-2&SFG-3	1274	733	541
	SFTB-1&SFTB-2&SFTB-3_vs_SFM-1&SFM-2&SFM-3	914	361	553

Table 1: Number of differentially expressed genes in four groups of cat

Figure3 (a)



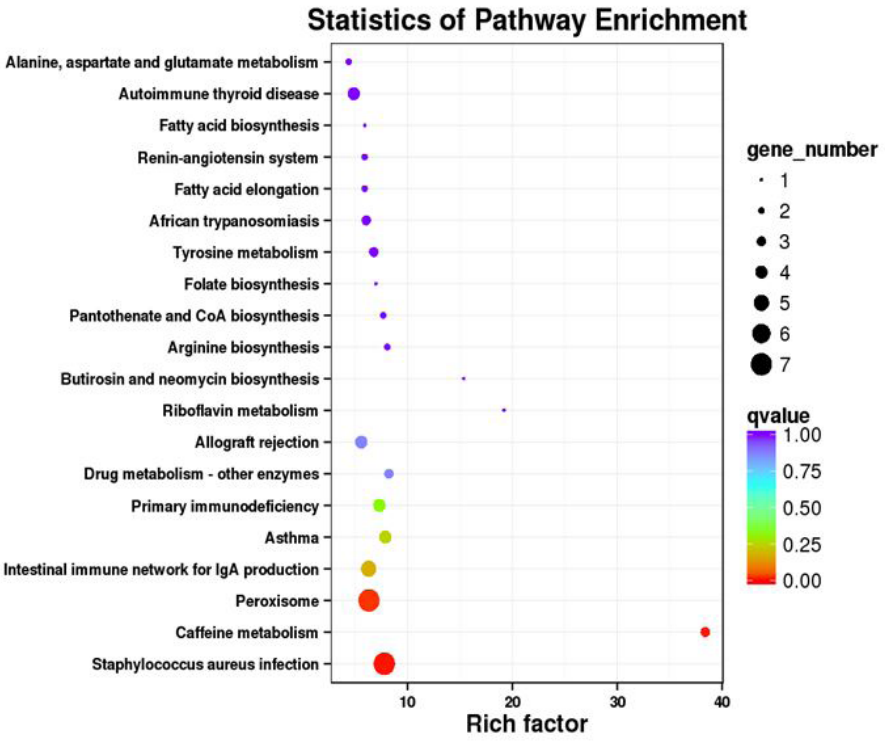
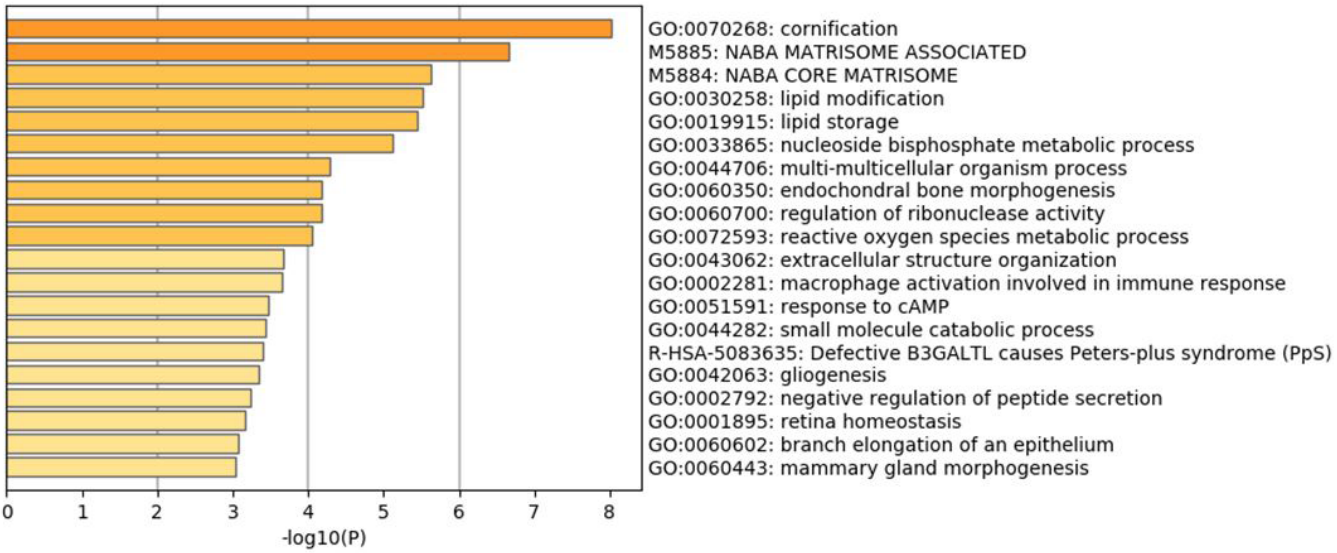

Statistics of Pathway Enrichment
Alanine, aspartate and glutamate metabolism
Autoimmune thyroid disease
Fatty acid biosynthesis
Renin-angiotensin system
Fatty acid elongation
African trypanosomiasis
Tyrosine metabolism
Folate biosynthesis
Pantothenate and CoA biosynthesis
Arginine biosynthesis
Butirosin and neomycin biosynthesis
Riboflavin metabolism
Allograft rejection
Drug metabolism - other enzymes
Primary immunodeficiency
Asthma
Intestinal immune network for IgA production
Peroxisome
Caffeine metabolism
Staphylococcus aureus infection
10
20
30
40
Rich factor
gene_number
1
2
3
4
5
6
7
qvalue
1.00
0.75
0.50
0.25
0.00

Figure 3 (b)


GO:0070268: cornification
M5885: NABA MATRISOME ASSOCIATED
M5884: NABA CORE MATRISOME
GO:0030258: lipid modification
GO:0019915: lipid storage
GO:0033865: nucleoside bisphosphate metabolic process
GO:0044706: multi-multicellular organism process
GO:0060350: endochondral bone morphogenesis
GO:0060700: regulation of ribonuclease activity
GO:0072593: reactive oxygen species metabolic process
GO:0043062: extracellular structure organization
GO:0002281: macrophage activation involved in immune response
GO:0051591: response to cAMP
GO:0044282: small molecule catabolic process
R-HSA-5083635: Defective B3GALTL causes Peters-plus syndrome (PpS)
GO:0042063: gliogenesis
GO:0002792: negative regulation of peptide secretion
GO:0001895: retina homeostasis
GO:0060602: branch elongation of an epithelium
GO:0060443: mammary gland morphogenesis
0
1
2
3
4
5
6
7
8
-log10(P)

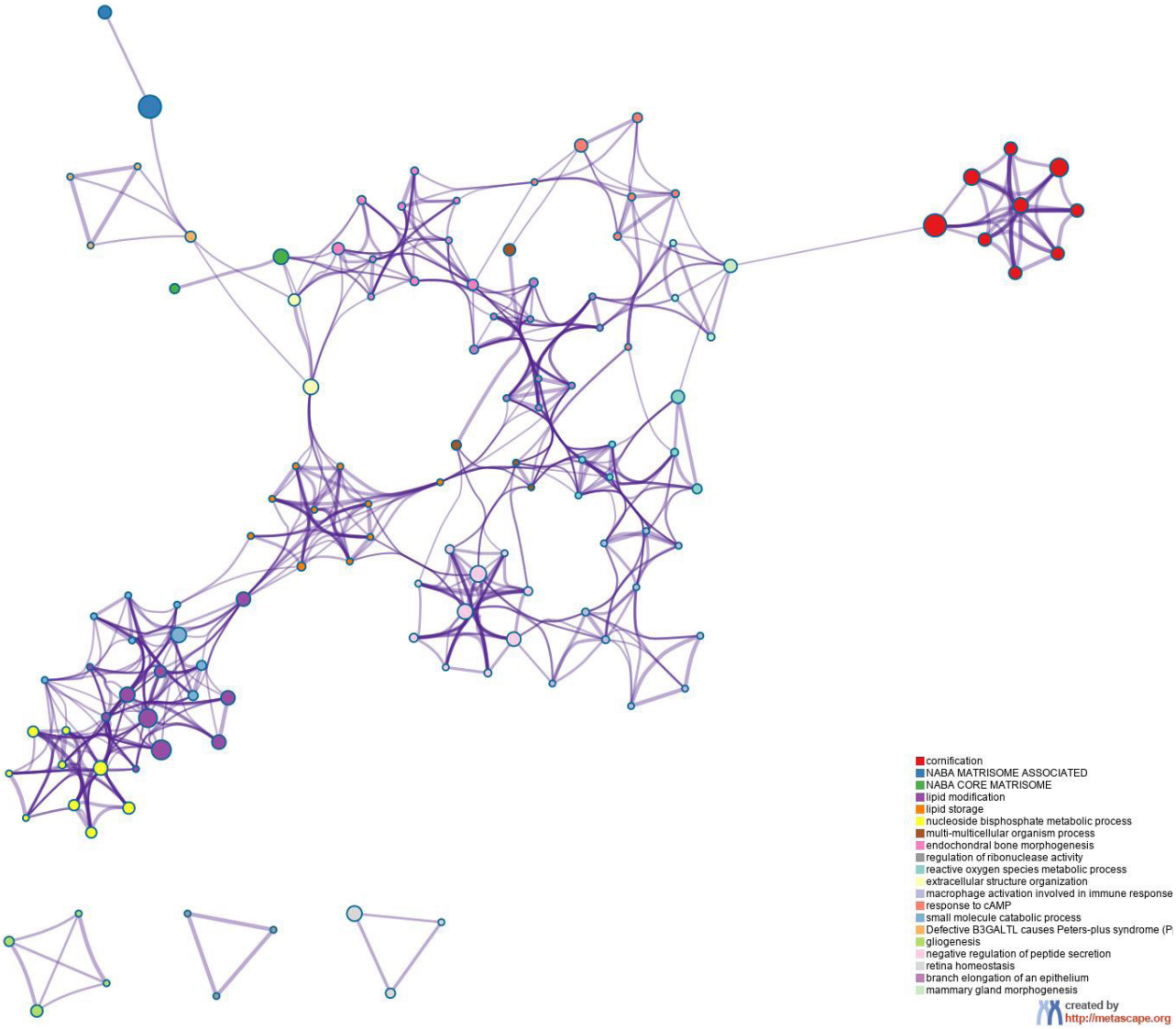


Figure 3: DGEs analysis of two groups of hairless cats compared with domestic cats in transcription. (a) The Veen set of DGEs with CK vs SFG and CK vs SFM. The first 20 signaling pathways in KEGG were enriched by 388 DGEs in the collection; (b) GO Classification Analysis with 388 DGEs. The x-coordinate is the p-value, and the y-coordinate is the enriched GO entry; (c) Enriched ontology clusters. Each term is represented by a circle node, where its size is proportional to the number of input genes that fall into that term, and its color represents its cluster identity

It was found that genes of the KRT family are mainly enriched in the items of "cornification," "NABA MATRISOME ASSOCIATED," "NABA CORE MATRISOME," "lipid modification," and so on. Through the enriched out dodgy clusters (http://metascape.org) of these genes (Fig. 3c), it is found that KRT family genes such as KRT73 and KRT40 are gathered.

Results of differential expression analysis of transcriptome genes in Sphynx cat group and Sphynx mutant cat group

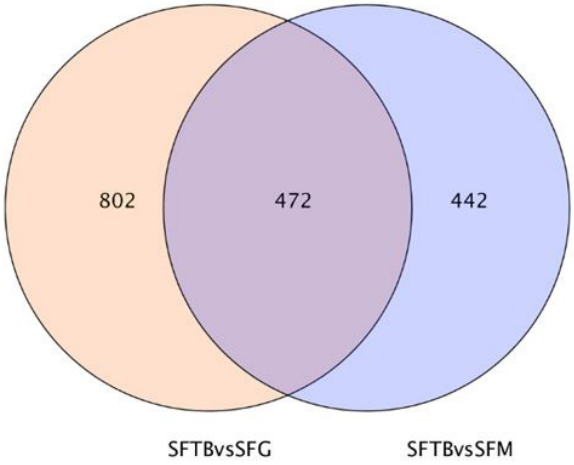
Through the Veen analysis of the pairwise comparison of SFG, SFM, and SFTB, it was found that there were 472 DGEs. Using the KEGG database (http://www.genome.jp/kegg/) analysis of the signal pathways of the first 20 DGEs, we found that DGEs were mainly enriched in pathways such as cell-adhesion molecules (CAMs), Morphine addiction, Antigen processing, and presentation (figure.4a).

The analysis of 472 DGEs by GO (http://metascape.org) showed that they were mainly enriched in items such as cornification, transport of inorganic cations, anions and amino acids, oligopeptides, protein nucleotide catabolic process (figure.4b).

After selecting the DGEs related to skin development for the cluster heat map, no significant differences were found among the three sample groups. Except for LOC101100432, which was downregulated in the SFTB group, all were up-regu-

lated. Besides, SFTB is clustered separately. Although no significant difference was found, it can be seen that SFTB is different from SFG and SFM in gene expression, while SFG and SFM show the same type of gene expression. (figure4c).

Figure 4 (a)



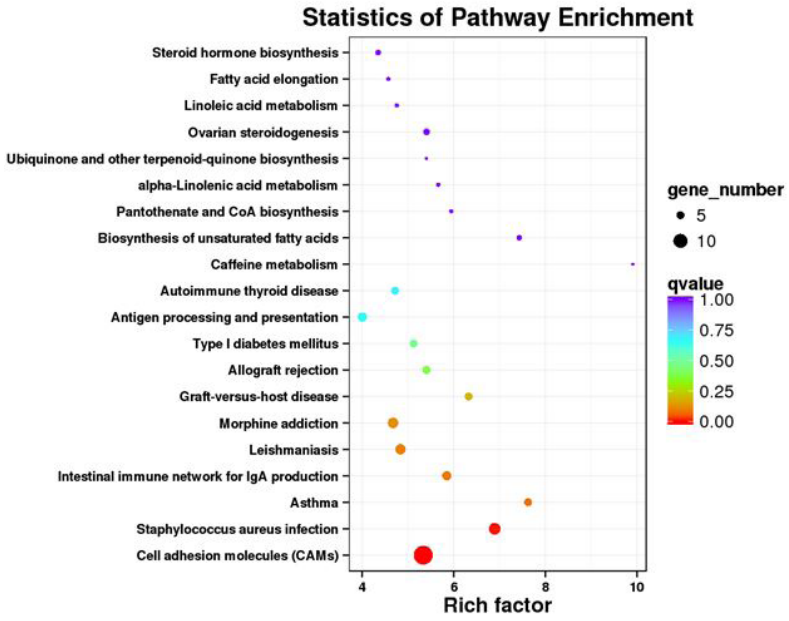
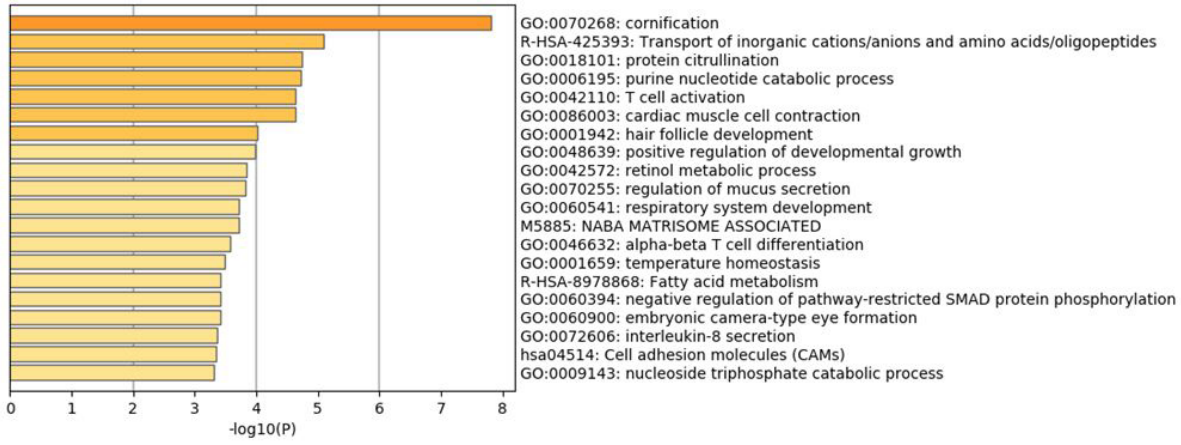


Figure.4 (b)



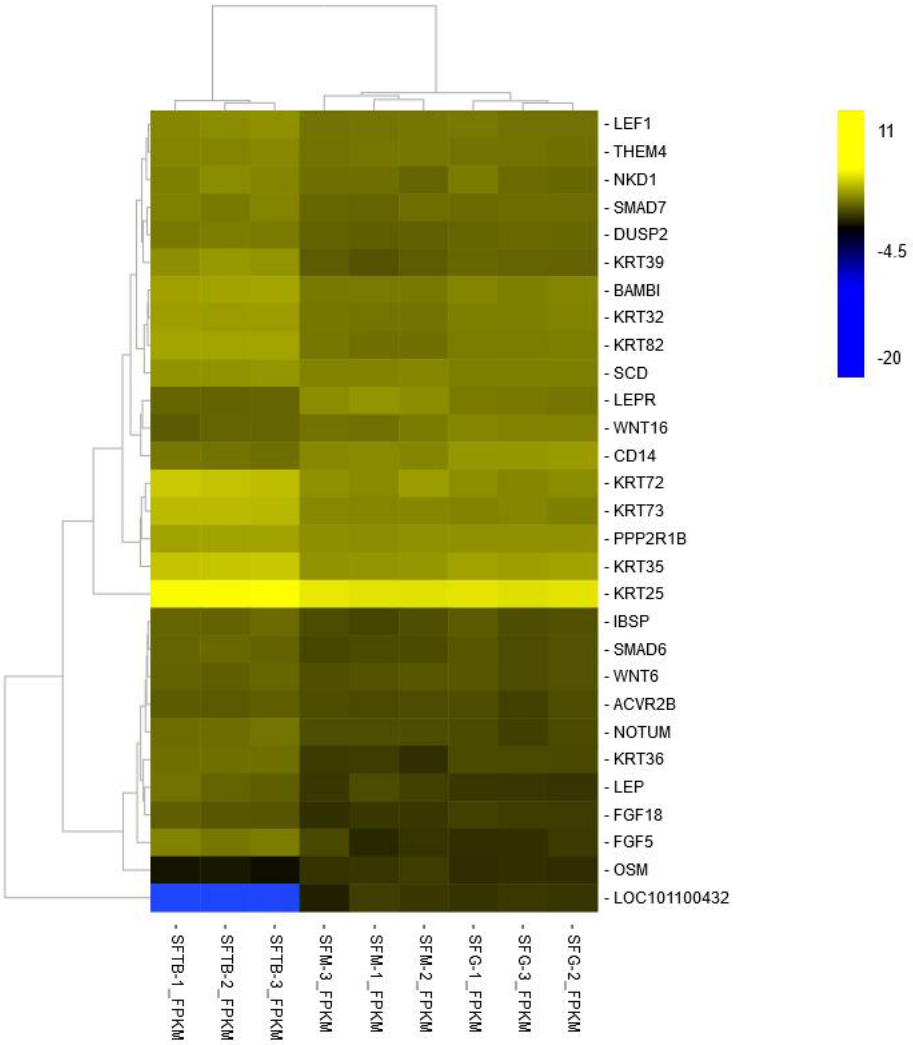


Figure 4: Two groups of hairless cat and hairless mutant cat transcripts were compared and analyzed for DGEs. (a) The Veen set of DGEs with SFTB vs SFG and SFTB vs SFM. The first 20 signaling pathways in KEGG were enriched by 388 DGEs in the collection; (b) GO classification analysis with 472 DGEs. The x-coordinate is the p-value, and the y-coordinate is the enriched GO entry; (c) The genes related to hair follicle development were selected from 472 genes for the cluster heat map. The x-coordinate represents the sample name and the clustering result of the sample, and the y-coordinate represents the differential genes and the clustering result of the gene. The different columns represent different samples, and the different rows represent different genes. Color represents the level of gene expression in the sample log10 (FPKM+0.000001)

Results of transcriptome differential expression gene analysis in four groups of cats

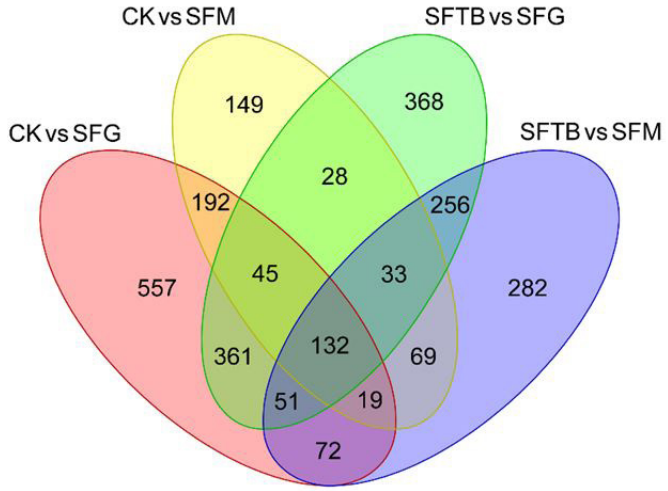
Four groups of cats (CK, SFG, SFM, and SFTB) were compared two by two. By Veen plots, we found that the resulting differential genes were found to be 132 DGEs in total (Supplementary Table 2).

Then, the expression pathways of these 132 DGEs were analysed through the KEGG database (Figure 5a).

Analysis of the GO database of 132 DGEs showed that they were mainly enriched in authentication, secondary metabolic processes, and cellular morphogenesis in neuronal differentiation (Figure 5b).

GO items associated with skin development were selected. Differentially expressed genes were analyzed, and clustered heat maps were drawn. Significant differences were found in ten genes, including KRT82, KRT32, KRT73, KRT35, KRT39, LEPR, NOTUM, KRT36, FGF18, and FGF5, which were transcribed from four groups of cat skin. Also, the gene expression patterns of CK and SFTB were the same, and the clustering was similar. KRT82, KRT32, KRT73, KRT35, and KRT39 were up-regulated, while LEPR, NOTUM, KRT36, and FGF18 were down-regulated. Meanwhile, the gene expression patterns of SFG and SFM were opposite to those of CK and SFTB (Figure. 5C).

Figure 5 (a)



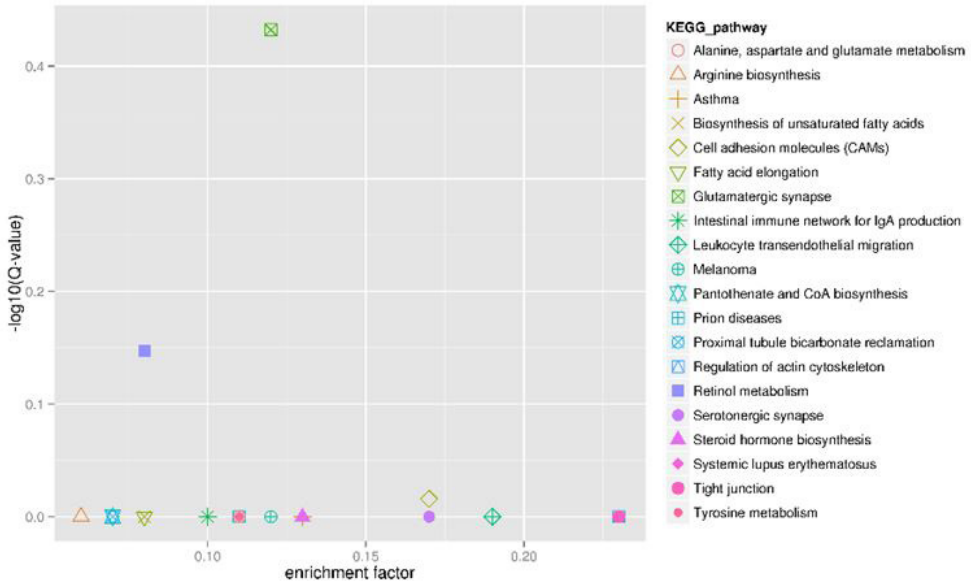


Figure5(b)



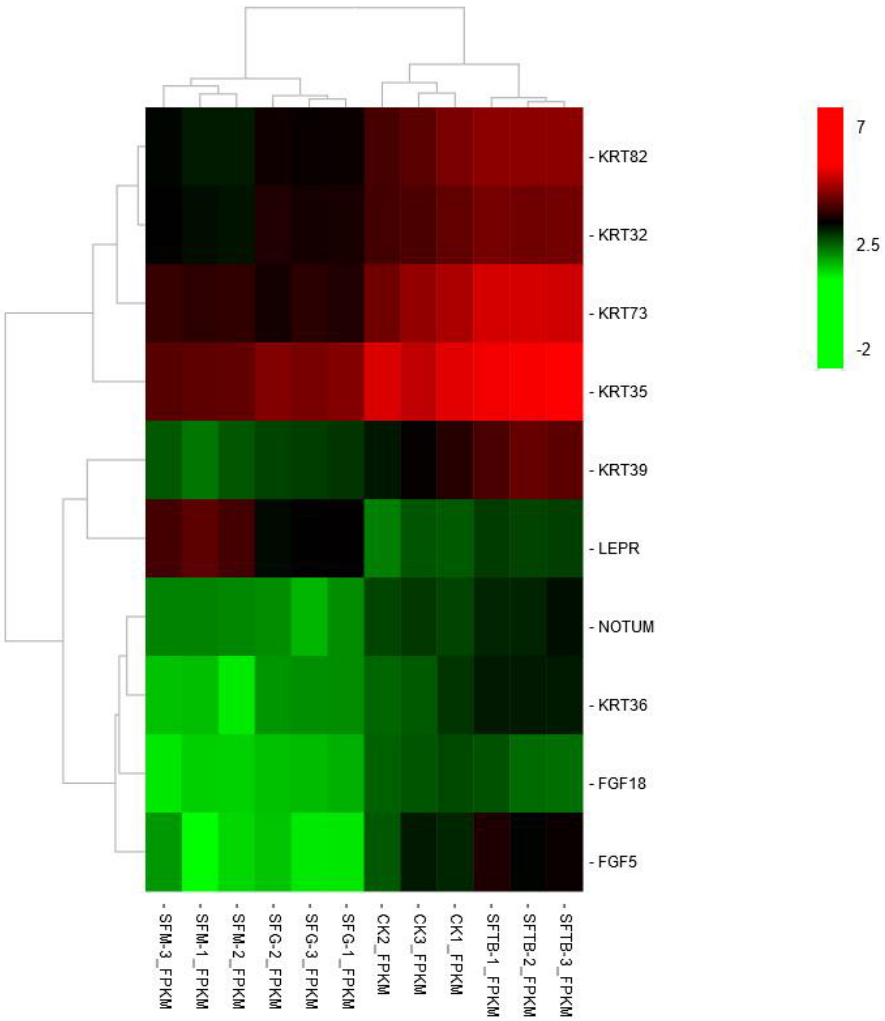


Figure 5: Different gene analysis of cat transcripts in four groups. The Veen set of DGEs with CK vs SFG CK vs SFM SFTB vs SFG and SFTB vs SFM. The first 20 signaling pathways in KEGG were enriched by 132 DGEs in the collection; (b) GO classification analysis with 132 DGEs; (c) The genes related to hair follicle development were selected from 132 genes for cluster heat map

qRT-PCR

To evaluate our DEG library, the relative expression levels of five DEGs from the KRT family (KRT37 KRT73, KRT32, KRT35, and KRT39), as well as FGF5, NOMTU, and FGF18 were analyzed by q-PCR. Overall, RNA-Seq results corroborated with the q-PCR results, as shown in Fig.6, demonstrating the reliability of our data.

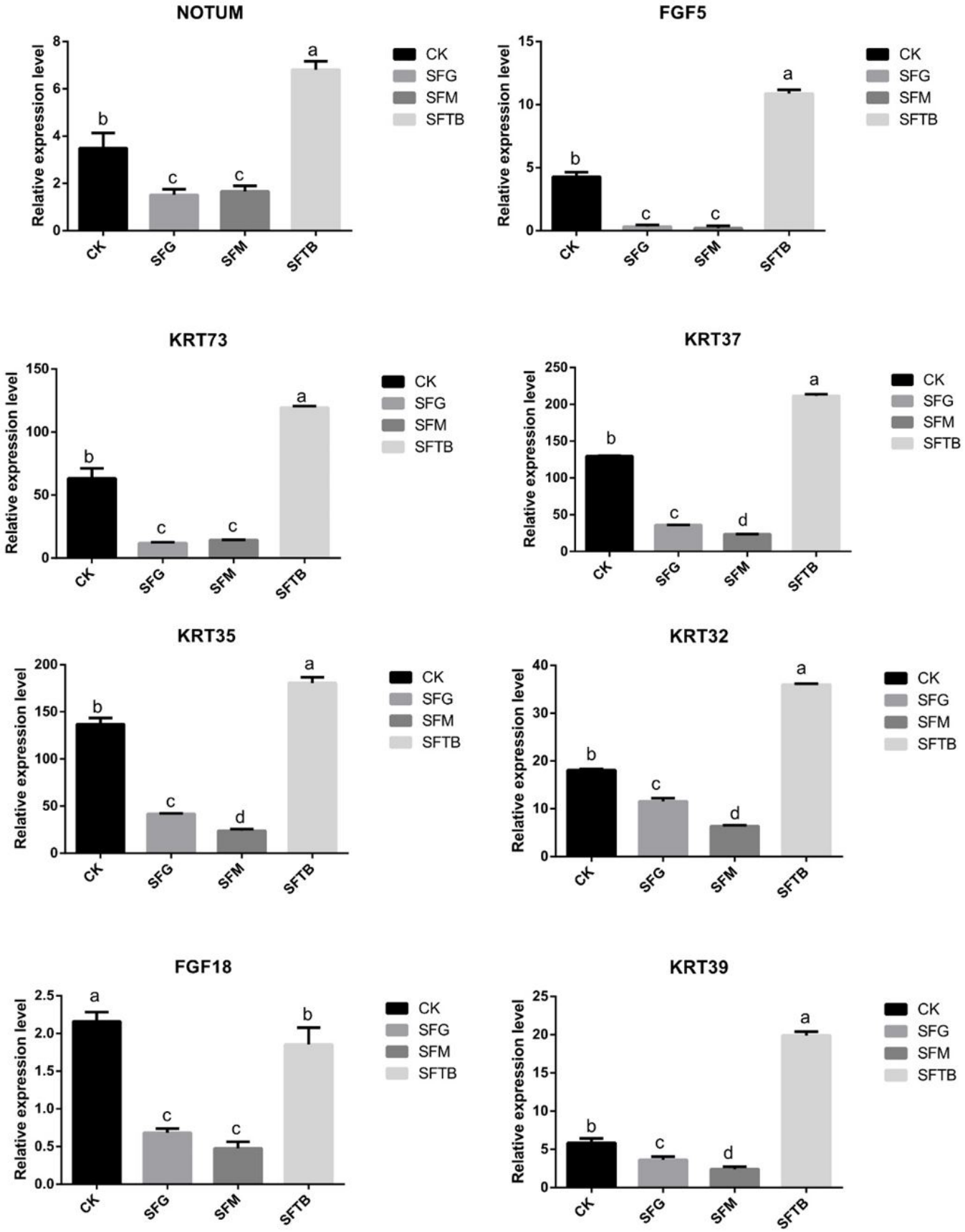


Figure 6: The q-PCR analysis of, 8 DEGs (NOTUM, FGF5, KRT37, KRT35, KRT32, KRT73, FGF18, and KRT39) of cat skin in four groups. The skin tissues of cats in four groups were collected. The q-PCR data were normalized with GAPDH as the reference gene. Bars represent standard error

Discussion

By comparing skin tissue transcriptions of mutated hairy Sphynx cats, Sphynx cats, and domestic cats through high throughput sequencing, this study has provided thought for analyzing the molecule mechanisms underlying hair growth difference. In this study, the clean data of all samples reach 6.23Gb and they verified that RNA-Seq data is qualified (Supplementary Table 1).

Heat map and principal component analysis of skin tissues showed that abundant of significant DEGs were found in Sphynx cats, mutated hairy Sphynx cats, and domestic cats. This means that DEGs may play essential roles in adjusting hair follicle development and hair growth. Heat map clustering analysis of these differentially expressed genes was performed by analyzing GO items related to skin development. The results revealed that ten genes, including KRT82, KRT32, KRT73, KRT35, KRT39, LEPR, NOTUM, KRT36, FGF18, and FGF5 h were significantly different in the skin transcript of these four groups of cats; hairy domestic cats were more similar to the mutated furry Sphynx cats, and hairless male Sphynx cats were more similar to hairless female Sphynx; in particular, genes KRT82, KRT32, KRT39, LEPR, and FGF5 had opposite expression patterns in both groups.

Keratin intermediate filament (KRT-IF) and keratin-associated protein genes encoded most of the hair protein [38,39]. According to the "The Naked Truth: Sphynx and Devon Rex cat breed mutations in KRT71", which describes that the KRT71 gene may be a candidate gene for Sphynx mutation, we synthesized the primer and amplified it. After sequencing, it was found that the Sphynx male cat, Sphynx female cat and kitten were only deleted at position 30 in the Exon7 primer amplification product, and the other sequencing results were the same (Supplementary Figure 1). As type II hair keratin, KRT82 can hybrid with type I keratin to form alkaline protein of hair and nails [40]; also, it has interactions with both KRT35 and KRT32 genes. Hair follicle [41] associated genes KRT34, KRT38, KRT39 are only expressed in the cortex, KRT40 and KRT84 are described in fibrous stratum corneum, KRT25 and type I KRT28 are represented in root-sheath [42]. In this study, genes associated with encoding keratin are expressed differentially in these four groups. Genes KRT82, KRT32 KRT39, KRT73, and KRT35 are up-regulated in domestic cats and mutated Sphynx cats. Except for KRT35, all the hairless groups are manifested as down-regulated. Assuming that the KRT genes can be involved in the ongoing activity of the hair follicle, then, these five KRT genes could promote hair growth, which needs to be verified later by reverse genetics and gene editing technologies.

In earlier reports, FGF5 was thought to be an inhibitor of hair growth in various mammalian species because it induces human hair follicles[43] to degrade. The CRISPR/Cas9 system is adopted to knock out and disrupt FGF5 in the body of a goat to make fiber become longer [43,44]. Many genetic types of research on animals with long hair have illustrated that gene FGF5 could destroy their expressions, thus prolonging the flourishing state of hair follicle development. As a result, the phenotypic trait of abnormally long hair appears. This phenomenon is generally called Angora mutation and has been verified in many species, including mice [45] hamsters [46] guinea pigs [47] rabbits [48] donkeys [49] goats [50] and sheep [51]. RNA-seq and q RT-PCR prove that the expression quantity of FGF5 in the bodies of hairy groups is higher than that in the hairless group. The gene expression is up-regulated, indicating that FGF5 polypeptide translated from the alternate splicing variants of FGF5 mRNA could inhibit the activity of FGF5 and promote hair growth. Therefore, it is speculated that FGF5s in FGF5 mRNA has restricted the movement of FGF5 and stimulated hair growth of cats. The functions of alternate splicing mutation of FGF5 in hair length need to be further studied.

Besides, the FGF5 gene is up-regulated in the expression of SFTB while down-regulated in the other three groups. In previous studies, Rosenquist [52] found that the behavior of the dermal papilla cells was changed by adding FGF5 protein in vitro culture. Ota [53] further found that FGF5 could inhibit skin hair growth by blocking the activity of dermal papilla cells. Suzuki et al. [54] discovered that FGF5 gene products could regulate rats' hair growth cycles through a synergistic effect. It is found by Ito et al. [51] that FGF-5S, a peptide translated by mRNA of alternative splicing, can antagonize the activity of FGF5 and promote skin hair growth, in which decapitated plays an important role. It is found that the depilation process of depleted mice with homozygous FGF5 ineffective allele (GO gene) is inhibited, indicating the regulatory effect of the GO gene on the hairless gene. Interestingly, KRT82 and KRT32 genes are down-regulated in Sphynx female cats while up-regulated in Sphynx male cats, which may be linked because both cats give birth to an offspring with hair.

GO analysis of differentially expressed genes in these four experimental groups revealed that most DEGs showed significant enrichment in biological processes such as certification,

secondary metabolic process, cell morphogenesis involved in neuron differentiation. The results suggest that these DEGs are potential regulators of hair follicle development and lipid metabolism. It is also found that the genes differentially expressed between the hairless group and mutant Sphynx cats all aggregate in the extracellular matrix (ECM)-receptor [55] interaction and basal-cell carcinoma pathway. Extracellular matrix in the EMC receptor interaction is a complex mixture of structural and functional macromolecular, including fibrous protein (collagen [56] fibronectin [57] and lignin [58]). Previous studies have shown that many EMC-related genes, including collagen, laminate, and fibronectin, are differentially expressed in primary and secondary hair follicle dermal papilla cells, resulting in enlarged dermal papilla [59]. Also, by analyzing DGEs in signal paths and MSPK [60] it is found that compared with hairless groups, LEF1, wnt11, NOTUM, and Wnt6 are upregulated in hairy groups.

In this study, transcriptional information from the skins of hairless Sphynx cats and mutant hairy Sphynx cats is obtained. Ten positively correlated genes were acquired through biological analysis, and the expressions of 8 genes were quantitatively measured. The results showed similar expression patterns. However, the immune system of mutant hairy Sphynx cats was not tested. In the following work, it is necessary to verify the functions of these ten genes in the vivo expressions of Sphynx cats and their relationship to the phenotype and to investigate the feasibility of taking hairless Sphynx cats as an animal model to study human hair diseases.

Declarations

Ethics approval and consent to participate

This study was approved by the Animal Ethics Committee of Qingdao Agricultural University. All operations were handled in strict accordance with the requirements for good animal practices of the Ethical Procedures and Guidelines for Animals of the People's Republic of China.

Consent for publication

Not applicable.

Availability of data and materials

The datasets used or analysed during the current study are available from the corresponding author on reasonable request.

Competing interests

The authors declare that they have no competing interests

Funding

Not applicable

Authors' contributions

Yanbo Yin contributed to the conception of the study; Xueting Qu, Wei Ge, Sen Wang performed the experiment; Xueting Qu, Minghui Zhao, Kunpeng Yuan, Yijun Han contributed significantly to analysis and manuscript preparation; Hao Zhou, Qingdong Luan, Haonan Qi, Ju Sun helped perform the analysis with constructive discussions; All authors reviewed the manuscript.

Acknowledgments

Thanks are due to My colleagues for assistance with the experiments and to Prof. Yin Y for valuable discussion.

References

1. Schmidt Küntzel A, Eizirik E, O'Brien SJ, Menotti Raymond M (2005) Tyrosinase and tyrosinase related protein 1 alleles specify domestic cat coat color phenotypes of the albino and brown loci. J Hered 96: 289-301.

2. Lyons LA, Imes DL, Rah HC, Grahn RA (2005) Tyrosinase mutations associated with Siamese and Burmese patterns in the domestic cat (Felis catus). Anim Genet 36: 119-26.

3. Kehler JS et al. (2007) Four independent mutations in the feline fibroblast growth factor 5 gene determine the long-haired phenotype in domestic cats. J Hered 98: 555-66.

4. Drögemüller C, Rüfenacht S, Wichert B, Leeb T (2007) Mutations within the FGF5 gene are associated with hair length in cats. Anim Genet 38: 218-21.

5. Cadieu E et al. (2009) Coat variation in the domestic dog is governed by variants in three genes. Science 326: 150-3.

6. Taylor LA, Harris MJ, Juriloff DM (2000) Whiskers amiss, a new vibrissae and hair mutation near the Krt1 cluster on mouse chromosome 11. Mamm Genome 11: 255-9.

7. Kuramoto T, Hirano R, Kuwamura M, Serikawa T (2010) Identification of the rat Rex mutation as a 7-bp deletion at splicing acceptor site of the Krt71 gene. J Vet Med Sci 72: 909-12.

8. Andl T, Reddy ST, Gaddapara T, Millar SE (2002) WNT signals are required for the initiation of hair follicle development. Dev Cell 2: 643-53.

9. Wang H, Zang C, Liu XS, Aster JC (2015) The role of Notch receptors in transcriptional regulation. J Cell Physiol 230: 982-8.

10. Brancaccio A et al. (2004) Requirement of the forkhead gene Foxe1, a target of sonic hedgehog signaling, in hair follicle morphogenesis. Hum Mol Genet 13: 2595-606.

11. Paladini RD, Saleh J, Qian C, Xu GX, Rubin LL (2005) Modulation of hair growth with small molecule agonists of the hedgehog signaling pathway. J Invest Dermatol 125: 638-46.

12. Widelitz RB et al. (2006) Distinct mechanisms underlie pattern formation in the skin and skin appendages. Birth Defects Res C Embryo Today 78: 280-91.

13. Garber M, Grabherr MG, Guttman M, Trapnell C (2011) Computational methods for transcriptome annotation and quantification using RNA-seq. Nat Methods 8: 469-77.

14. Montagna MT, De Giglio O, Agodi A, Pasquarella C (2017) Response to Comments on Montagna et al. "Evaluation of Legionella Air Contamination in Healthcare Facilities by Different Sampling Methods: An Italian Multicenter Study" Int. J. Environ. Res. Public Health 2017, 14, 670. Int J Environ Res Public Health 14.

15. Nowak JA, Polak L, Pasolli HA, Fuchs E (2008) Hair follicle stem cells are specified and function in early skin morphogenesis. Cell Stem Cell 3: 33-43.

16. Ouspenskaia T, Matos I, Mertz AF, Fiore VF, Fuchs E (2016) WNT-SHH Antagonism Specifies and Expands Stem Cells prior to Niche Formation. Cell 164: 156-69.

17. Ezratty EJ et al. (2011) A role for the primary cilium in Notch signaling and epidermal differentiation during skin development. Cell 145: 1129-41.

18. James K, Hosking B, Gardner J, Muscat GE, Koopman P (2003) Sox18 mutations in the ragged mouse alleles ragged-like and opossum. Genesis 36: 1-6.

19. Schneider MR (2012) Genetic mouse models for skin research: strategies and resources. Genesis 50: 652-64.

20. Vassar R, Rosenberg M, Ross S, Tyner A, Fuchs E (1989) Tissue-specific and differentiation-specific expression of a human K14 keratin gene in transgenic mice. Proc Natl Acad Sci U S A 86: 1563-7.

21. Byrne C, Fuchs E (1993) Probing keratinocyte and differentiation specificity of the human K5 promoter in vitro and in transgenic mice. Mol Cell Biol 13: 3176-90.

22. Ji YZ, Bai Y, Wang S, Li FQA (2015) KRT1 gene mutation related to epidermolytic ichthyosis in a Chinese family. Clin Exp Dermatol 40: 879-82.

23. Hotz A et al. (2016) Expanding the Clinical and Genetic Spectrum of KRT1, KRT2 and KRT10 Mutations in Keratinopathic Ichthyosis. Acta Derm Venereol 96: 473-8.

24. Miyachi K et al. (2018) Extracellular proteoglycan decorin maintains human hair follicle stem cells. J Dermatol 45: 1403-10.

25. Tirado CA, Sebastian S, Moore JO, Gong JZ, Goodman BK (2005) Molecular and cytogenetic characterization of a novel rearrangement involving chromosomes 9, 12, and 17 resulting in ETV6 (TEL) and ABL fusion. Cancer Genet Cytogenet 157: 74-7.

26. Olsen EA, Whiting DA (2019) Focal atrichia: A diagnostic clue in female pattern hair loss. J Am Acad Dermatol 80: 1538-43. e1531.

27. Florea L, Song L, Salzberg SL (2013) Thousands of exon skipping events differentiate among splicing patterns in sixteen human tissues. F1000Res 2: 188.

28. Anders S, Huber W (2010) Differential expression analysis for sequence count data. Genome Biol 11: R106.

29. Altschul SF et al. (1997) Gapped BLAST and PSI-BLAST: a new generation of protein database search programs. Nucleic Acids Res 25: 3389-402.

30. Cartwright J, Atz T, Newman S, Mueller M, Demirci JR (2017) Integrative Review of Interventions to Promote Breastfeeding in the Late Preterm Infant. J Obstet Gynecol Neonatal Nurs 46: 347-56.

31. UniProt Consortium T (2018) UniProt: the universal protein knowledgebase. Nucleic Acids Res 46: 2699.

32. Ashburner M et al. (2000) Gene ontology: tool for the unification of biology. The Gene Ontology Consortium. Nat Genet 25: 25-9.

33. Tatusov RL, Galperin MY, Natale DA, Koonin EV (2000) The COG database: a tool for genome-scale analysis of protein functions and evolution. Nucleic Acids Res 28: 33-6.

34. Koonin EV et al. (2004) A comprehensive evolutionary classification of proteins encoded in complete eukaryotic genomes. Genome Biol 5: R7.

35. Finn RD et al. (2014) Pfam: the protein family's database. Nucleic Acids Res 42: D222-30.

36. Kanehisa M, Goto S, Kawashima S, Okuno Y, Hattori M (2004) The KEGG resource for deciphering the genome. Nucleic Acids Res 32: D277-80.

37. Froussios K, Mourão K, Simpson G, Barton G, Schurch N (2019) Relative Abundance of Transcripts (RATs): Identifying differential isoform abundance from RNA-seq. F1000Res 8: 213.

38. Sulayman A et al. (2018) Association analysis of polymorphisms in six keratin genes with wool traits in sheep. Asian-Australas J Anim Sci 31: 775-83.

39. Coulombe PA, Omary MB (2002) 'Hard' and 'soft' principles defining the structure, function and regulation of keratin intermediate filaments. Curr Opin Cell Biol 14: 110-22.

40. Yu Z et al. (2011) Annotation of sheep keratin intermediate filament genes and their patterns of expression. Exp Dermatol 20: 582-8.

41. Obara K et al. (2019) Hair-follicle-associated pluripotent stem cells derived from cryopreserved intact human hair follicles sustain multilineage differentiation potential. Sci Rep 9: 9326.

42. Li C et al. (2018) Trio-Based Deep Sequencing Reveals a Low Incidence of Off-Target Mutations in the Offspring of Genetically Edited Goats. Front Genet 9: 449.

43. Wang X et al. (2016) Correction: Disruption of FGF5 in Cashmere Goats Using CRISPR/Cas9 Results in More Secondary Hair Follicles and Longer Fibers. PLoS One 11: e0167322.

44. Dierks C, Mömke S, Philipp U, Distl O (2013) Allelic heterogeneity of FGF5 mutations causes the long-hair phenotype in dogs. Anim Genet 44: 425-31.

45. Mizuno S et al. (2011) Retrotransposon-mediated Fgf5(go-Utr) mutant mice with long pelage hair. Exp Anim 60: 161-7.

46. Yoshizawa Y et al. (2015) A 1-bp deletion in Fgf5 causes male-dominant long hair in the Syrian hamster. Mamm Genome 26: 630-7.

47. Yu F et al. (2018) A nonsense mutation in the FGF5 gene is associated with the long-haired phenotype in domestic guinea pigs (Cavia porcellus). Anim Genet 49: 269.

48. Li CX, Jiang MS, Chen SY, Lai SJ (2008) Correlation analysis between single nucleotide polymorphism of FGF5 gene and wool yield in rabbits. Yi Chuan 30: 893-9.

49. Legrand R, Tiret L, Abitbol M (2014) Two recessive mutations in FGF5 are associated with the long-hair phenotype in donkeys. Genet Sel Evol 46: 65.

50. Wang X et al. (2016) Disruption of FGF5 in Cashmere Goats Using CRISPR/Cas9 Results in More Secondary Hair Follicles and Longer Fibers. PLoS One 11: e0164640.

51. Ito C et al. (2003) Decapeptide with fibroblast growth factor (FGF)-5 partial sequence inhibits hair growth suppressing activity of FGF-5. J Cell Physiol 197: 272-83.

52. Rosenquist TA, Martin GR (1996) Fibroblast growth factor signalling in the hair growth cycle: expression of the fibroblast growth factor receptor and ligand genes in the murine hair follicle. Dev Dyn 205: 379-86.

53. Ota Y et al. (2002) Fibroblast growth factor 5 inhibits hair growth by blocking dermal papilla cell activation. Biochem Biophys Res Commun 290: 169-76.

54. Suzuki S et al. (1998) Localization of rat FGF-5 protein in skin macrophage-like cells and FGF-5S protein in hair follicle: possible involvement of two Fgf-5 gene products in hair growth cycle regulation. J Invest Dermatol 111: 963-72.

55. Najafi M, Farhood B, Mortezaee K (2019) Extracellular matrix (ECM) stiffness and degradation as cancer drivers. J Cell Biochem 120: 2782-90.

56. Ricard-Blum S (2011) The collagen family. Cold Spring Harb Perspect Biol 3: a004978.

57. Pankov R, Yamada KM (2002) Fibronectin at a glance. J Cell Sci 115: 3861-3.

58. Boerjan W, Ralph J (2003) Baucher, M. Lignin biosynthesis. Annu Rev Plant Biol 54: 519-46.

59. Madaan A, Verma R, Singh AT, Jaggi M (2018) Review of Hair Follicle Dermal Papilla cells as in vitro screening model for hair growth. Int J Cosmet Sci 40: 429-50.

60. Clark RR, Dierckman B, Sampatacos N, Snyder S (2013) Biomechanical performance of traditional arthroscopic knots versus slippage-proof knots. Arthroscopy 29: 1175-81.

Supplementary Tables

Table 1

Samples	Clean reads	Clean bases	GC Content	Q30≤%
CK1	24,493,333	7,319,806,086	52.01%	93.87%
CK2	21,023,691	6,278,953,946	52.94%	93.75%
CK3	20,997,651	6,270,901,280	52.36%	93.85%
SFG1	22,431,265	6,690,446,576	51.01%	93.95%
SFG2	21,460,498	6,407,452,926	51.25%	93.34%
SFG3	22,152,945	6,608,229,856	50.29%	93.84%
SFM1	20,915,160	6,245,008,740	50.39%	94.11%
SFM2	21,080,338	6,289,054,760	50.18%	94.43%
SFM3	21,714,075	6,483,986,272	50.83%	94.12%
SFTB1	21,226,037	6,335,513,780	52.05%	94.02%
SFTB2	20,929,481	6,251,523,716	52.13%	93.90%
SFTB3	20,891,499	6,231,446,938	51.10%	94.47%

Table 2: qPCR primer

primer	**primer sequence 5'-3'**	**TM**
NOTUM-F	AAGGAATCCAAGGGCAGTCG	60
NOTUM-R	AGTTCTCCCGGTTGAAGCAG	60
KRT35-F	TACTCCCGAGGCAGCCAG	60
KRT35-R	GTTGCCGGGAAGACCAAGTA	60
FGF18-F	TATTGTCCGCTGCAAGCTGT	60
FGF18-R	GAGCAATGCAGGGTCACTTG	60
KRT39-F	GTCCCAGAGGGTTTCAGTCAAT	60
KRT39-R	GGCTAGATGCTTTGCCCTGG	60
FGF5-F	TGGAGCAGAGCAGTTTCCAG	60
FGF5-R	GGTAAATTTGGCTTAACATATTGGC	60
KRT32-F	AAGTTGCCCTGTAACCCGTG	60
KRT32-R	TGAGGGACTTTCAGTAGCGG	60
KRT73-F	AGTGCAAGCGAATTCAAGGAC	60
KRT73-R	GGGAGTCCAGAGGAAACCAG	60
KRT37-F	AGAGCGAGGACTGCAAACTC	60
KRT37-R	TCCTAACTCGGGCCTTCAGA	60

Submit your manuscript to a JScholar journal and benefit from:

- Convenient online submission
- Rigorous peer review
- Immediate publication on acceptance
- Open access: articles freely available online
- High visibility within the field
- Better discount for your subsequent articles

Submit your manuscript at
http://www.jscholaronline.org/submit-manuscript.php